ARTICLE

BIOTECHNOLOGY and BIOENGINEERING

The Continuum Heterogeneous Biofilm Model With Multiple Limiting Substrate Monod Kinetics

Elio Emilio Gonzo,[1] Stefan Wuertz,[2,3,4] Veronica B. Rajal[1]

[1]INIQUI (CONICET)—Facultad de Ingeniería, Universidad Nacional de Salta, Av. Bolivia 5150, Salta 4400, Argentina; telephone: +54-387 425 1006; fax: +54-387 425 1006; e-mail: gonzo@unsa.edu.ar

[2]School of Biological Sciences, Singapore Centre on Environmental Life Sciences Engineering (SCELSE), Nanyang Technological University, Singapore, Singapore

[3]School of Civil and Environmental Engineering, Nanyang Technological University, Singapore, Singapore

[4]Department of Civil and Environmental Engineering, University of California, Davis, Davis, California

ABSTRACT: We describe a novel procedure to estimate the net growth rate of biofilms on multiple substrates. The approach is based on diffusion-reaction mass balances for chemical species in a continuum biofilm model with reaction kinetics corresponding to a Double-Monod expression. This analytical model considers a heterogeneous biofilm with variable distributions of biofilm density, activity, and effective diffusivity as a function of depth. We present the procedure to estimate the effectiveness factor analytically and compare the outcome with values obtained by the application of a rigorous numerical computational method using several theoretical examples and a test case. A comparison of the profiles of the effectiveness factor as a function of the Thiele modulus, ϕ, revealed that the activity of a homogeneous biofilm could be as much as 42% higher than that of a heterogeneous biofilm, under the given conditions. The maximum relative error between numerical and estimated effectiveness factor was 2.03% at ϕ near 0.7 (corresponding to a normalized Thiele modulus $\phi^* = 1$). For $\phi < 0.3$ or $\phi > 1.4$, the relative error was less than 0.5%. A biofilm containing aerobic ammonium oxidizers was chosen as a test case to illustrate the model's capability. We assumed a continuum heterogeneous biofilm model where the effective diffusivities of oxygen and ammonium change with biofilm position. Calculations were performed for two scenarios; Case I had low dissolved oxygen (DO) concentrations and Case II had high DO concentrations, with a concentration at the biofilm–fluid interface of 10 g O_2/m^3. For Case II, ammonium was the limiting substrate for a biofilm surface concentration, C_{Ns}, $\leq$13.84 g of N/m^3. At these concentrations ammonium was limiting inside the biofilm, and oxygen was fully penetrating. Conversely, for $C_{Ns} > 13.84$ g of N/m^3, oxygen became the limiting substrate inside the biofilm and ammonium was fully penetrating. Finally, a generalized procedure to estimate the effectiveness factor for a system with multiple ($n > 2$) limiting substrates is given.

Biotechnol. Bioeng. 2014;111: 2252–2264.

KEYWORDS: biofilm model; effectiveness factor; continuum heterogeneous biofilm; multiple-substrate limitation; Monod kinetics

Introduction

Biofilms are complex microbial ecosystems in which several physical, chemical, and biological processes take place simultaneously (Wanner, 1995). Both the physical structure of biofilms (Lewandowski et al., 2007) and the dynamics of key microbial populations, such as nitrifying bacteria versus general heterotrophic bacteria, have been well studied experimentally. Appropriate methods include fluorescent in situ hybridization coupled with confocal laser scanning microscopy, magnetic resonance imaging, scanning transmission X-ray microscopy (Behrens et al., 2012; Neu et al., 2010), environmental scanning electron microscopy (Alhede et al., 2012), microsensors (Gonzalez et al., 2011; Kofoed et al., 2012), and microautoradiography (Collins et al., 2007; Nielsen and Nielsen, 2005). One-dimensional models are available to simulate processes in biofilms, especially at the bioreactor scale, but are often considered too simplistic in biofilm biology. Yet the growing number of multidimensional mathematical models used to describe mass transfer and reactions in biofilms are often inaccessible

Correspondence to: E.E. Gonzo

Contract grant sponsor: CONICET
Contract grant sponsor: Universidad Nacional de Salta in Argentina
Contract grant sponsor: Fogarty International Center at the University of California, Davis, USA
Contract grant sponsor: Singapore Ministry of Education and National Research Foundation
Received 3 December 2013; Revision received 31 March 2014; Accepted 7 May 2014
Accepted manuscript online 2 June 2014;
Article first published online 18 July 2014 in Wiley Online Library (http://onlinelibrary.wiley.com/doi/10.1002/bit.25284/abstract).
DOI 10.1002/bit.25284

to experimentally oriented researchers (Wanner et al., 2006; Wuertz et al., 2003) because they (i) describe hypothetical rather than experimental biofilms, (ii) the physical and hydrodynamic conditions in experimental biofilms are insufficiently characterized, or (iii) the numerical simulation techniques are not available to the experimentalists. It is, therefore, of interest to consider analytical approaches to advanced biofilm modeling (Gonzo et al., 2012) that may be more amenable to many researchers, especially those in the life sciences.

All models make simplifying assumptions and parameter values describing the kinetics and stoichiometry of the metabolic processes taking place in the bioreactor (the net biofilm growth rate) are necessary. Biofilms are represented either as homogeneous or heterogeneous systems; these latter models are needed for many experimental studies where a continuum (rather than uniform) biofilm density must be assumed. In the continuum heterogeneous model, the biofilm is treated as a continuous phase where the phenomena mediated by microorganisms, densely packed in micro-colonies separated by interstitial voids, are lumped in an effective mass transfer (effective diffusivity) and a net biofilm growth rate. This model considers that both the effective diffusivity of the substrate and the biofilm density vary along the coordinate normal to the biofilm surface (Beyenal and Lewandowski, 2005; Gonzo et al., 2012).

Although modeling microbial growth with one limiting substrate, such as in the Monod equation, is a common practice, microorganisms often consume multiple substances from the environment for their growth. Yet when it cannot be guaranteed that only one substrate is rate limiting throughout the entire biofilm compartment, the concentrations of multiple substrates must be solved simultaneously (Wanner et al., 2006). Therefore, the extension of the one-substrate model to a multiple-substrate analysis is needed for practical applications (Noguera et al., 1999; Wanner and Gujer, 1986). The term "dual-limitation kinetics" refers to a type of multiple-substrate limitation in which the substrates together limit the overall biomass growth rate. In the case of two substrates, three different models, the multiplicative or interacting model (Double-Monod), the non-interacting model, and the additive model, are frequently used to describe the effects of dual limitation on cell-growth (Bae and Rittmann, 1996; Bungay, 1994; Wu et al., 2007). The multiplicative model assumes that both nutrients limit the overall growth rate:

$$r = q_{\max}\left(\frac{C_A}{K_A + C_A}\right)\left(\frac{C_B}{K_B + C_B}\right) \quad (1)$$

where r is the specific cell-growth rate, $q_{\max}$ is the maximum specific cell-growth rate, C_A and C_B are the two limiting substrates concentrations, and K_A and K_B are the half-maximum-rate concentrations for substrates A and B, respectively. The multiplicative model (Bae and Rittmann, 1996) may be found from a special case of enzyme-substrate reactions in which two substrates react together at the active sites of one enzyme to produce a single product. Both substrates bind the single enzyme to form an [A-Enzyme-B] intermediate.

The non-interactive model (Odencrantz, 1992) postulates that the microbial growth of a microorganism is limited only by the more severely limiting substrate, while the other substrate has no effect on the kinetics. In this case, Equation (1) can be simplified to single substrate Monod kinetics. On the other hand, in the additive or weighted model, the growth rate is expressed by weighting the contributions of individual nutrient limitations (Bungay, 1994).

The effectiveness factor, η, is the ratio between the diffusion-limited substrate consumption rate and the substrate consumption rate that is not limited by diffusion. Therefore, by calculating the effectiveness factor, it is possible to estimate the net rate of substrate consumption and the net biofilm growth rate. In a previous work (Gonzo et al., 2012), we developed a procedure to estimate analytically the effectiveness factor, considering different biofilm heterogeneities as well as different values for the Monod half-maximum-rate concentration constant for a single substrate. This approach allows easy computation of η in a computer program and, consequently, the rate of substrate utilization can be determined under many different conditions resulting from biofilm heterogeneity.

The aims of this study were (i) to describe the procedure to estimate the effectiveness factor for multiplicative Double-Monod kinetics, (ii) to generalize the procedure for multiple limiting substrate kinetics in a continuum heterogeneous biofilm, and (iii) to analyze the behavior of these systems using a test case.

Materials and Methods

Model Formulation

The continuous heterogeneous biofilm considers that both substrate diffusivity and biofilm density change with depth in the direction normal to the biofilm surface (Gonzo et al., 2012). For dual-substrate Monod kinetics, the concentration profiles of both substrates, A and B (Fig. 1), should be considered. Taking into account that the substrate effective diffusivities and the biofilm density vary with the position in the biofilm, the mass balances for the nutrients, at steady state, are given by:

$$\frac{d}{dx}D_{fA}(x)\frac{dC_A}{dx} = \frac{q_{\max}}{Y_A}X_f(x)\left(\frac{C_A}{K_A + C_A}\right)\left(\frac{C_B}{K_B + C_B}\right) \quad (2)$$

$$\frac{d}{dx}D_{fB}(x)\frac{dC_B}{dx} = \frac{q_{\max}}{Y_B}X_f(x)\left(\frac{C_A}{K_A + C_A}\right)\left(\frac{C_B}{K_B + C_B}\right) \quad (3)$$

where D_{fA} and D_{fB} are the effective diffusivities of the substrates, X_f is the biofilm density, and Y_A and Y_B are the biomass yield coefficients of the substrates A and B, respectively.

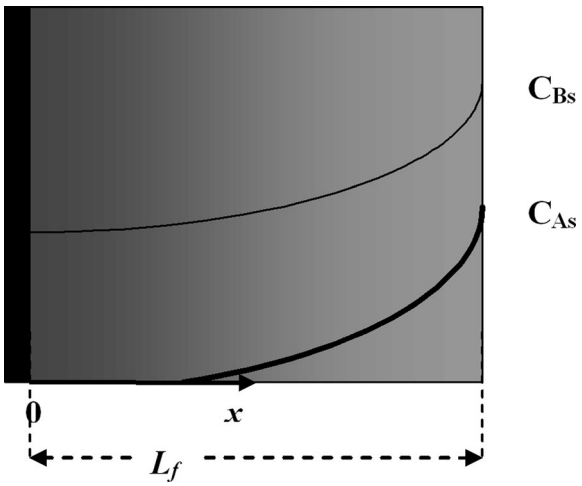

Figure 1. Structure of the continuum heterogeneous biofilm model with concentration profiles for substrates A and B. Lf, biofilm thickness.

The following assumptions were made in Equations (2) and (3):

a. The biofilm is a continuum.
b. Substrate is transferred by diffusion only (Fick's law).
c. Microorganisms consume the substrates at a rate according to Double-Monod kinetics.
d. Biofilm density and substrate effective diffusivities change in the x direction.
e. Steady state (pseudo-steady state) of substrate consumption applies. The rates of substrate consumption are fast compared to the rate of biofilm growth.
f. External resistances to mass transfer are neglected. Therefore, the substrate concentrations at the biofilm-fluid interface are known, namely, C_{As} and C_{Bs}.
g. The substratum (support where the biofilm grows) is impermeable.

Under these conditions, the appropriate boundary conditions for Equations (2) and (3) are:

$$\text{At} \quad x = L_f \quad C_A = C_{As} \quad \text{and} \quad C_B = C_{Bs} \tag{4}$$

$$\text{At} \quad x = 0 \quad \frac{dC_A}{dx} = 0 \quad \text{and} \quad \frac{dC_B}{dx} = 0 \tag{5}$$

$D_{fA}(x)$, $D_{fB}(x)$, and $X_f(x)$ Profiles

The variation of substrate effective diffusivity as a function of distance from the substratum (x) can be approximated by a linear relation, as shown by experimental studies (Beyenal and Lewandowski, 2000, 2002, 2005; Beyenal et al., 1998; Lewandowski and Beyenal, 2003). For the substrate A, the relation is:

$$D_{fA}(x) = \alpha_A + \xi x \tag{6}$$

Parameters α_A and ξ (Gonzo et al., 2012) depend on the substrate concentration and flow velocity at which biofilms are grown. Similarly, the dependence of D_{fB} with x is:

$$D_{fB}(x) = \alpha_B + \xi x \tag{7}$$

Fan et al. (1990) found the following empirical correlation between relative diffusivity $\left(D^{\circ}_{fA}\right)$ and biofilm density:

$$D^{\circ}_{fA}(x) = 1 - \frac{0.43X_f^{0.92}}{11.19 + 0.27X_f^{0.99}} \tag{8}$$

where

$$D^{\circ}_{fA}(x) = \frac{D_{fA}(x)}{D_{wA}} \tag{9}$$

D_{wA} is the diffusivity of substrate A in the liquid medium. The higher the density of the biofilm, the less pore volume is available to the substrate to diffuse through the biofilm.

Dimensionless Equations for the System

Let us define the following dimensionless parameters and dimensionless Double-Monod half rate constants, β_A and β_B:

$$x^* = \frac{x}{L_f} \quad C_A^* = \frac{C_A}{C_{As}} \quad C_B^* = \frac{C_B}{C_{Bs}} \quad \beta_A = \frac{K_A}{C_{As}} \quad \beta_B = \frac{K_B}{C_{Bs}}$$
$$r^* = \frac{r}{r_s} \quad D_{fA}^* = \frac{D_{fA}}{\bar{D}_{fA}} \quad D_{fB}^* = \frac{D_{fB}}{\bar{D}_{fB}} \quad X_f^* = \frac{X_f}{\bar{X}_f} \tag{10}$$

where

$$r_s = q_{max}\left(\frac{C_{As}}{K_A + C_{As}}\right)\left(\frac{C_{Bs}}{K_B + C_{Bs}}\right) \tag{11}$$

r_s is the reference reaction rate since all the variables are known.

The parameters $\bar{D}_{fA}$ and $\bar{D}_{fB}$ are the average effective diffusivities of substrates A and B, respectively, and $\bar{X}_f$ is the average biofilm density across the total biofilm.

Assuming substrate A is the limiting substrate and after introducing these dimensionless parameters in Equations (2) and (3), the following differential equations are found:

$$\frac{d}{dx^*}D_{fA}^*\frac{dC_A^*}{dx^*} = \phi^2 X_f^* r^*\left(C_A^*, C_B^*\right) \tag{12}$$

$$\frac{d}{dx^*}D_{fB}^*\frac{dC_B^*}{dx^*} = \phi^2 \Gamma_B X_f^* r^*\left(C_A^*, C_B^*\right) \tag{13}$$

where

$$r^*\left(C_A^*, C_B^*\right) = (\beta_A + 1)(\beta_B + 1)\left(\frac{C_A^*}{\beta_A + C_A^*}\right)\left(\frac{C_B^*}{\beta_B + C_B^*}\right) \tag{14}$$

The Thiele modulus, ϕ, is the ratio between a reference reaction rate in a homogeneous biofilm, which is not

diffusion limited and has a density equal to the average value in the biofilm, and the diffusion rate ϕ, is given as:

$$\phi^2 = \frac{L_f^2}{\bar{D}_{fA} C_{As}} \frac{q_{max}}{Y_A} \bar{X}_f \left(\frac{C_{As}}{K_A + C_{As}}\right)\left(\frac{C_{Bs}}{K_B + C_{Bs}}\right) = \frac{L_f^2 \bar{X}_f}{\bar{D}_{fA} C_{As} Y_A} r_s \quad (15)$$

and the parameter Γ_B as:

$$\Gamma_B = \nu_B \frac{C_{As} \bar{D}_{fA}}{C_{Bs} \bar{D}_{fB}} \quad (16)$$

Γ_B relates stoichiometric coefficients, average substrate effective diffusivities, and biofilm–fluid interface concentrations. Therefore, Γ_B plays an important role in determining which substrate becomes limiting.

The stoichiometric coefficient linking the utilization of limiting substrates *A* and *B* can be found as follows (Wanner et al., 2006):

$$\frac{1}{Y_B} = \frac{1 - Y_A}{Y_A} \quad \text{Therefore,} \quad \nu_B = \frac{Y_A}{Y_B} = (1 - Y_A) \quad (17)$$

where ν_B represents the ratio of the stoichiometric coefficients for substrates A and B.

The dimensionless boundary conditions for the differential Equations (12) and (13) are as follows:

$$\text{At} \quad x^* = 1 \quad C_A^* = 1 \quad C_B^* = 1 \quad (18)$$

$$\text{At} \quad x^* = 0 \quad \frac{dC_A^*}{dx^*} = 0 \quad \frac{dC_B^*}{dx^*} = 0 \quad (19)$$

Beyenal and Lewandowski (2000) found that the variation of effective diffusivity across the biofilm is constant. We assume that this diffusivity gradient (ξ) is constant for any of the substrates studied here since it is related to the biofilm heterogeneity. Consequently, the ratio between $\bar{D}_{fA}$ and $\bar{D}_{fB}$, and between D_{fA} and D_{fB}, remains almost constant (see test case). Therefore,

$$D_{fA}^*(x^*) \cong D_{fB}^*(x^*) \quad (20)$$

Taking into account Equation (20) and dimensionless boundary conditions (18) and (19), the relation between C_A^* and C_B^* is found by solving Equations (12) and (13):

$$C_B^* = \Gamma_B \left(C_A^* - 1\right) + 1 \quad (21)$$

The necessary condition for substrate A to be the limiting substrate is that Γ_B should be lower than one. In this case, the concentration profiles for C_A and C_B in the biofilm will be those shown in Figure 1.

According to Equation (16) a linear relation can be found between the substrate concentrations at the limit ($\Gamma_B = 1$) where the limiting component changes. This relation is:

$$C_{Bs} = \left[\nu_B \frac{\bar{D}_{fA}}{\bar{D}_{fB}}\right] C_{As} \quad (22)$$

This means that if $\Gamma_B < 1$ the limiting substrate will be A, whereas if $\Gamma_B > 1$ then *B* becomes the limiting component (see Fig. 4).

According to Equations (14) and (21), the dimensionless reaction rate r^* will be a function only of limiting substrate concentration C_A^*:

$$r^*\left(C_A^*\right) = (\beta_A + 1)(\beta_B + 1) \times \frac{C_A^*}{(\beta_A + C_A^*)} \frac{\left[\Gamma_B\left(C_A^* - 1\right) + 1\right]}{\left[\beta_B + \Gamma_B\left(C_A^* - 1\right) + 1\right]} \quad (23)$$

Also

$$\left(\frac{dr^*}{dC_A^*}\right)_{C_A^* = 1} = r^{*\prime}(1) = \frac{\beta_A}{(\beta_A + 1)} + \frac{\Gamma_B \beta_B}{(\beta_B + 1)} \quad (24)$$

To solve the differential Equation (12), it is necessary to know the relationships of D_{fA}^* and X_f^* with the dimensionless coordinate x^*.

Introducing the dimensionless parameters,

$$\Psi = \frac{\alpha_A}{L_f \xi} \quad (25)$$

and

$$\kappa = \frac{D_w}{\alpha_A} \quad (26)$$

following Beyenal and Lewandowski (2005) and Gonzo et al. (2012), and considering that the average effective diffusivity in the biofilm $\left(\bar{D}_{fA}\right)$ is equal to

$$\bar{D}_{fA} = \alpha_A + \frac{\xi L_f}{2} \quad (27)$$

the functions of D_{fA}^* and X_f^* with x^* are found:

$$D_{fA}^*(x^*) = \frac{2(\Psi + x^*)}{2\Psi + 1} = c\left(1 + \frac{x^*}{\Psi}\right) \quad (28)$$

and

$$X_f^*(x^*) = \frac{-38.856 + 38.976\kappa^{0.7782}(1 + (x^*/\Psi))^{-0.7782}}{\bar{X}_f} = \frac{a + b(1 + (x^*/\Psi))^{-0.7782}}{\bar{X}_f} \quad (29)$$

where the parameters are: $a = -38.856$, $b = 38.976$, and $c = ((2\Psi)/(2\Psi + 1))$.

Effectiveness Factor Estimation

We previously defined the effectiveness factor, η, as the ratio between the observed limiting substrate consumption rate (r_{Aob}) (rate of reaction with diffusion resistance) and the substrate consumption rate without diffusion limitation (r_{As}) (Gonzo et al., 2012) after Bischoff and Froment (1980).

$$\eta = \frac{r_{Aob}}{r_{As}} = \int_0^1 X_f^* r^* \left(C_A^*\right) dx^* \tag{30}$$

It follows that the observed reaction rate (r_{Aob}) can be directly obtained from Equation (30). In addition, the key nutrient steady-state mass balance at the biofilm–fluid interface gives:

$$D_{fA}(x = L_f)\left.\frac{dC_A}{dx}\right|_{x=L_f} = S_x = \eta \frac{q_{max}}{Y_A} \frac{C_{As}}{(K_A + C_{As})} \frac{C_{Bs}}{(K_B + C_{Bs})} S_x L_f \tag{31}$$

where S_x is the biofilm–fluid interface area.

Considering the dimensionless variables and parameters previously defined, Equation (31) yields:

$$\frac{D_{fA}^*(1)}{\phi^2}\left(\frac{dC_A^*}{dx^*}\right)_{x^*=1} = \eta \tag{32}$$

Although either Equation (30) or (32) could be used to estimate η, this is not possible here because $C_A^*(x^*)$ is not known. Instead Equation (12) can be solved approximately by a perturbation procedure (Gottifredi and Gonzo, 1986) when $\phi \ll 1$ or when $\phi \gg 1$, using a matching expression to find the analytical solution for η. This procedure was successfully applied in estimating the effectiveness factor for a continuum heterogeneous biofilm and Monod kinetics with a single limiting substrate (Gonzo et al., 2012). Its application to dual limiting substrate Monod kinetics is given in Supplemental Material A.

Matching Expression for the Effectiveness Factor

The matching expression for the estimation of the effectiveness factor for the entire range of Thiele modulus (ϕ) values is given by (Gonzo and Gottifredi, 2007):

$$\eta = [\phi^{*2} + \exp(-d\,\phi^{*2})]^{-(1/2)} \tag{33}$$

where

$$\rho = \left(2D_{fA}^*(1)X_f^*(1)I\right)^{1/2} \quad \sigma = \frac{b\Psi^2}{\bar{X}_f^2 c(0.2218)} r^{*\prime}(1)(F) \tag{34}$$

with

$$\phi^* = \frac{\phi}{\rho} \quad d = 1 - 2\sigma^* \quad \sigma^* = \sigma\rho^2 \tag{35}$$

By definition, if parameter d is found to be lower than zero, then $d = 0$ applies.

Extension of Method From Dual to Multiple Monod Kinetics

The generalization for n substrate ($n > 2$) Monod kinetics is given in Supplemental Material B.

Computational Methods

The finite elements method was used for the numerical solution of differential Equation (12) with analytical Equation (23), using the boundary conditions presented in Equations (18) and (19). The commercial software used to obtain numerical results with the finite element method was ABAQUS (http://www.3ds.com/products-services/simulia/portfolio/abaqus/overview/) with several improvements carried out by the research group at the Centro Internacional de Métodos Numéricos en Ingeniería (CIMNE, Universidad Politécnica de Cataluña, Barcelona, España—Universidad Nacional de Salta, Facultad de Ingeniería, Salta, Argentina).

Results

Relationship of the Effectiveness Factor With Thiele Modulus and parameters κ, Ψ, β_A, and β_B

A comparison of the profiles of the effectiveness factor as a function of the Thiele modulus in a continuum heterogeneous biofilm (with $\beta_A = 0.4$, $\beta_B = 2$, $\Gamma_B = 0.5$, $\Psi = 0.5$, and $\kappa = 4$) and in a homogeneous biofilm ($\beta_A = 0.4$, $\beta_B = 2$, $\Gamma_B = 0.5$, and $X_f^* = D_{fA}^* = D_{fB}^* = 1$) revealed that the activity of a homogeneous biofilm could be as much as 42% higher than that of a heterogeneous biofilm, under the given conditions (Fig. 2). The figure also shows the effectiveness factor values that were obtained numerically using the finite element method (Zienkewicz and Taylor, 1991). The maximum relative error between numerical and estimated effectiveness factor was 2.03% at a Thiele modulus near 0.7 (corresponding to a normalized Thiele modulus $\phi^* = 1$). For $\phi < 0.3$ or $\phi > 1.4$, the relative error was less than 0.5%.

The influence of parameters κ and Ψ, which are directly related to biofilm heterogeneity, on the effectiveness factor, is shown in Figure 3a and b. As expected from Equations (25) and (26), the effective diffusivity gradient, ξ, is inversely proportional to κ and Ψ. Therefore, if κ or Ψ increases the gradient decreases and the solution tends toward a homogenous biofilm.

It is interesting to analyze the effect of parameters β_A on η for Double-Monod kinetics. Taking into account the expression of the dimensionless reaction rate

$$r^*\left(C_A^*, C_B^*\right) = (\beta_A + 1)(\beta_B + 1)\left(\frac{C_A^*}{\beta_A + C_A^*}\right)\left(\frac{C_B^*}{\beta_B + C_B^*}\right)$$

we can find the effect of parameter β_A on the effectiveness factor for constant values of β_B, Γ_B, Ψ, and κ (Fig. 3c).

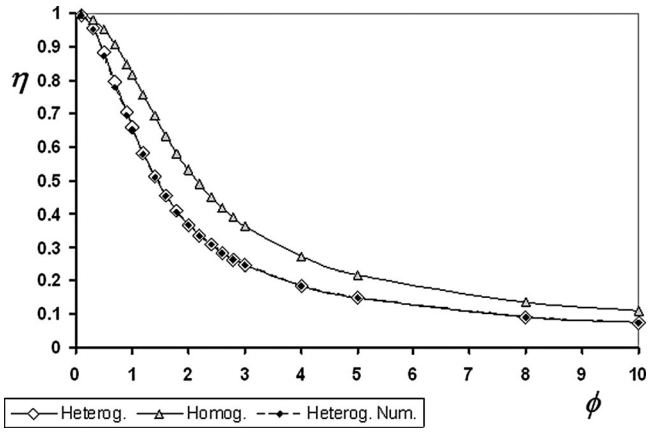

Figure 2. Comparison between effectiveness factors considering homogeneous and continuous heterogeneous biofilms and corresponding factors after numerical simulation for: $\beta_A = 0.4$, $\beta_B = 2$, $\Gamma_B = 0.5$, $\Psi = 0.5$, $\kappa = 4$. η(Heterog.), Equation (33) with $\rho = 0.7386$ and $d = 0.4211$; η(Homog.), Equation (33) with $\rho = 1.0919$ and $d = 0.5080$.

When β_A takes on very small values (at high substrate A concentrations), $\beta_A \to 0$. Then

$$(\beta_A + 1) \to 1 \quad \text{and} \quad \left(\beta_A + C_A^*\right) \to C_A^* \tag{36}$$

Therefore,

$$r^*\left(C_A^*, C_B^*\right) \approx (\beta_B + 1)\left(\frac{C_B^*}{\beta_B + C_B^*}\right) \tag{37}$$

The kinetics approach a single substrate Monod expression for substrate B and a zero-order reaction for substrate A.

If instead β_A takes on high values (at low substrate A concentrations), $\beta_A \to \infty$

$$(\beta_A + 1) \to \beta_A \quad \text{and} \quad \left(\beta_A + C_A^*\right) \to \beta_A \tag{38}$$

Equation (14) becomes

$$r^*\left(C_A^*, C_B^*\right) \approx (\beta_B + 1) C_A^*\left(\frac{C_B^*}{\beta_B + C_B^*}\right) \tag{39}$$

Here, the reaction rate approaches single Monod kinetics for substrate B and first-order kinetics for substrate A. In both situations, the kinetics are independent of the value of parameter β_A and, therefore, of the effectiveness factor η. This effect of parameter β_A on η is clearly observed in Figure 3c where the effectiveness factor is plotted as a function of β_A, at a constant value of the Thiele modulus. It can be seen that η tends toward a constant value for high and low values of the parameter β_A. The same situation is found when we analyze

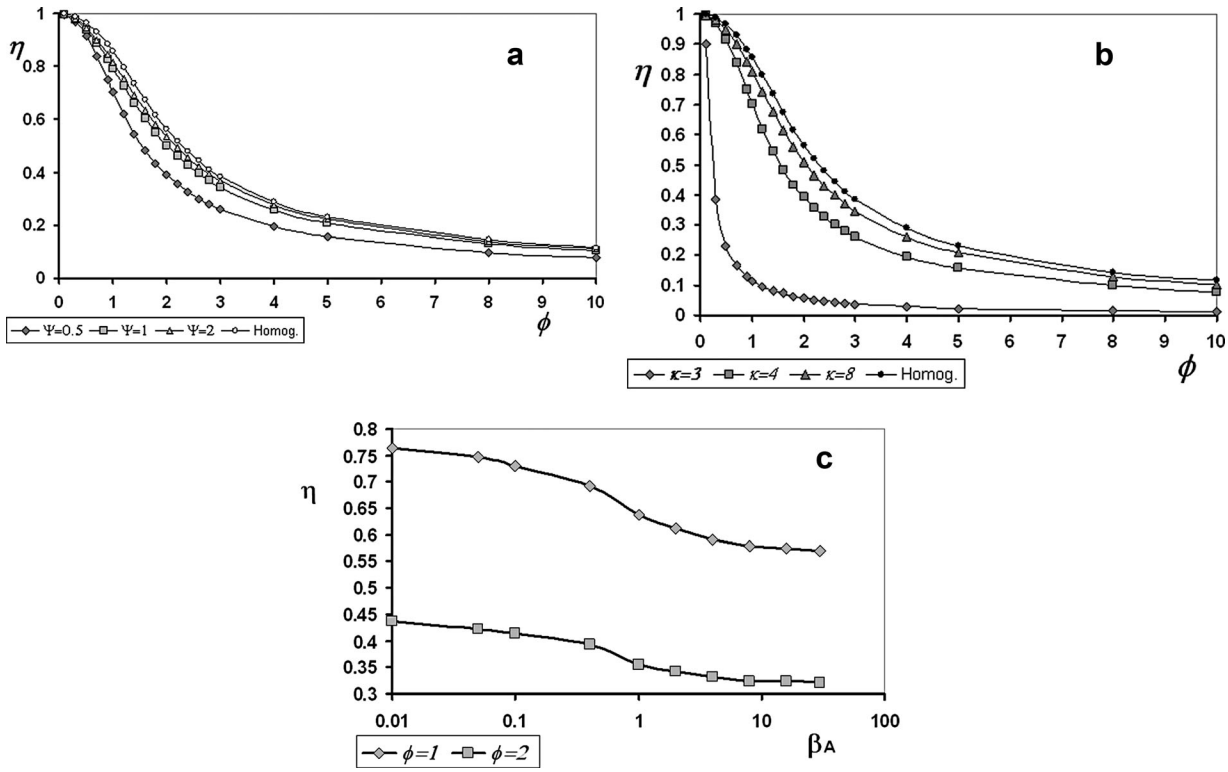

Figure 3. Effect of parameters Ψ, κ, and β_A on the effectiveness factor for Double-Monod kinetics with: (**a**) $\beta_A = 0.4$, $\beta_B = 0.7$, $\Gamma_B = 0.25$, $\kappa = 4$; (**b**) $\beta_A = 0.4$, $\beta_B = 0.7$, $\Gamma_B = 0.25$, $\Psi = 0.5$; (**c**) constant value of the Thiele modulus; $\beta_B = 0.8$, $\Gamma_B = 0.5$, $\Psi = 0.5$, $\kappa = 4$.

Table I. Kinetics and parameters used in the model assuming a biofilm growing at 30°C that contains aerobic ammonium oxidizers.

Model parameter[a]	Designation	Value[b]
Maximum specific growth rate	q_{max}	2.05 per day
Oxygen saturation constant	K_O	0.6 g of O_2/m^3
Ammonium saturation constant	K_N	2.4 g of N/m^3
Yield of ammonium oxidizer on ammonium	Y_N	0.15 g of biomass/g of N
Physical properties		
Oxygen average diffusion coefficient	$\bar{D}_{fO}$	2.0×10^{-4} m^2/day
Ammonium average diffusion coefficient	$\bar{D}_{fN}$	1.7×10^{-4} m^2/day
Average value of biomass density in biofilm	$\bar{X}_f$	10,000 g biomass/m^3 biofilm
Biofilm thickness	L_f	300 μm
Biofilm heterogeneity	Ψ	0.5
Relation $D_{wO}/\alpha_O \approx D_{wN}/\alpha_N$	κ	4

[a]Kinetic model: $r = q_{max} X_f \frac{C_N}{K_N + C_N} \frac{C_O}{K_O + C_O} \left(\frac{\text{g of biomass}}{m^3_{\text{biofilm}}\ \text{day}} \right)$.

[b]Values taken from Picioreanu et al. (2004).

the effect of parameter β_B at constant values of β_A, Γ_B, Ψ, and κ (results not shown).

Case Study

A biofilm containing aerobic ammonium oxidizers was chosen as a test case to illustrate the model's capability, with the kinetic values and parameters (Table I) taken from Picioreanu et al. (2004). The effectiveness factor, η, was calculated using Equation (33) for the limiting substrate with rate expressions and parameters given in Tables I–III. Parameters σ and ρ are those given by Equations (A-9) and (A-18), respectively. Thus, the observed (net) rate of the limiting substrate consumption or biomass production for a given value of the biofilm thickness is found. We assumed a continuum heterogeneous biofilm model where the effective diffusivities of oxygen and ammonium change with biofilm position (x) according to:

$$\begin{aligned} D_{fO} &= 10^{-4} + 0.666x \\ D_{fN} &= 0.85 \times 10^{-4} + 0.666x \end{aligned} \tag{40}$$

The biofilm density, in (g/m^3), changes as a function of dimensionless position x^* (Gonzo et al., 2012) as follows:

$$X_f = -11980 + 12011\kappa^{0.7782} \left(1 + \frac{x^*}{\Psi} \right)^{-0.7782} \tag{41}$$

After applying these equations of effective diffusivities of oxygen and ammonium and the biofilm density as a function of biofilm position, the calculated average values of the effective diffusivities and biofilm density agreed with the values given in Table I for a continuum heterogeneous biofilm consisting of aerobic ammonium oxidizers.

Test Conditions

Calculations were performed for two scenarios; Case I had low dissolved oxygen (DO) concentrations (Table II) and Case II had high DO concentrations (Table III). Figure 5 presents the observed reaction of biomass production r_{bio} (g of biomass/$m^3$of biofilm/h) for both cases, as function of the substrate concentration C_{Ns}, in the range where either oxygen or ammonium is the limiting substrate. For this test case Equation (22), which relates the substrate concentrations where the limiting component changes, becomes:

$$C_{Os} = 0.7225 C_{Ns} \tag{42}$$

For a given value of the oxygen surface concentration, ammonia will be the limiting substrate for concentrations below the value on the straight line shown in Figure 4. For ammonia concentrations higher than that, oxygen will become the limiting component. Likewise, for a given value of ammonia surface concentration, oxygen will be the limiting substrate for concentrations below the value given by the linear Equation (42). For oxygen concentrations higher than that, ammonia becomes the limiting substrate.

Case I

Low oxygen concentration: $C_{Os} = 2$ g of O_2/m^3 (corresponds to an oxygen partial pressure of 0.055 atm).

According to Equation (42) oxygen is the limiting component (oxygen is potentially limiting inside the biofilm) provided

$$\Gamma_N = \frac{1}{1 - Y_N} \frac{C_{Os} \bar{D}_{fO}}{C_{Ns} \bar{D}_{fN}} \leq 1 \tag{43}$$

For the limiting situation, $\Gamma_N = 1$, oxygen will be the limiting component for $C_{Ns} > 2.77$ g of N/m^3. Ammonium is fully penetrating the biofilm (Fig. 4).

Case II

High oxygen concentration: $C_{Os} = 10$ g of O_2/m^3 (corresponds to an oxygen partial pressure of 0.28 atm).

According to Equation (42), ammonium is the limiting component (ammonium substrate is limiting inside

Table II. Calculated parameters for test Case I: oxygen-limited process.

$$C_{0s} = 2\,\text{g of } O_2/\text{m}^3 \quad \beta_0 = 0.3$$

$$I = (\beta_0 + 1)(\beta_N + 1)\int_0^1 \frac{C_0^*}{\beta_0 + C_0^*}\frac{\left[\Gamma_N(C_0^* - 1) + 1\right]}{\left[\beta_N + \Gamma_N(C_0^* - 1) + 1\right]}\,dC_O^*$$

$$r_{0s} = q_{max}\frac{(1 - Y_N)}{Y_N}\bar{X}_f\left[\frac{C_{0s}}{K_0 + C_{0s}}\right]\left[\frac{C_{Ns}}{K_N + C_{Ns}}\right]$$

$$r^{*\prime}(1) = \frac{\beta_0}{\beta_0 + 1} + \frac{\Gamma_N\beta_N}{\beta_N + 1} \quad \phi^2 = \frac{L_f^2}{\bar{D}_{f0}C_{0s}}r_{0s}$$

	C_{Ns} (g/m^3)						
Parameters	3	5	8	12	15	17	19
β_N	0.8000	0.4800	0.3000	0.2000	0.1600	0.1412	0.1263
Γ_N	0.9227	0.5536	0.3460	0.2307	0.1845	0.1628	0.1457
$r^{*\prime}(1)$	0.6409	0.4104	0.3107	0.2692	0.2563	0.2509	0.2471
r_{Os} (g O_2/m^3 day)	4,9643.9	60,377.7	68,737.7	74,465.8	77,033.6	78,304.3	79,337.4
I	0.5517	0.6597	0.7001	0.7153	0.7198	0.7216	0.7229
ϕ^2	11.17	13.58	15.47	16.75	17.33	17.62	17.85
ρ	0.7094	0.7756	0.7990	0.8077	0.8102	0.8112	0.8120
ϕ^*	4.708	4.757	4.919	5.064	5.134	5.178	5.203
d	0.3818	0.5267	0.6199	0.633	0.6775	0.6835	0.6877
η	0.212	0.210	0.203	0.196	0.195	0.193	0.192
r_{ob} (O_2) (g O_2/m^{3}day)	10,544.4	12,691.4	13,953.7	14,595.3	15,004.6	15,112.7	15,232.8
r_{bio} (g biomass/m^{3}h)	77.53	93.32	102.60	107.32	110.30	111.10	112.00

r_{Os} (g O_2/m^3 day): rate of oxygen consumption evaluated on the biofilm–fluid interface.
r_{ob} (O_2) (g O_2/m^3 day): net rate of oxygen consumption in the biofilm.
r_{bio} (g biomass/m^3 h): net rate of biomass growth in the biofilm.

Table III. Calculated parameters for test Case II: ammonium-limited process.

$$C_{0s} = 10\,\text{g of } O_2/\text{m}^3 \quad \beta_0 = 0.06$$

$$I = (\beta_0 + 1)(\beta_N + 1)\int_0^1 \frac{C_N^*}{\beta_N + C_N^*}\frac{\left[\Gamma_0(C_N^* - 1) + 1\right]}{\left[\beta_0 + \Gamma_0(C_N^* - 1) + 1\right]}\,dC_N^*$$

$$r_{Ns} = \frac{q_{max}}{Y_N}\bar{X}_f\left[\frac{C_{0s}}{K_0 + C_{0s}}\right]\left[\frac{C_{Ns}}{K_N + C_{Ns}}\right]$$

$$r^{*\prime}(1) = \frac{\beta_N}{\beta_N + 1} + \frac{\Gamma_0\beta_0}{\beta_0 + 1} \quad \phi^2 = \frac{L_f^2}{\bar{D}_{fN}C_{Ns}}r_{Ns}$$

	C_{Ns}(g/m^3)						
Parameters	2	4	7	10	13	13.84	15 (*)
β_N	1.2000	0.6000	0.3428	0.2400	0.1846	0.1734	0.1600
Γ_O	0.1445	0.2890	0.5057	0.7225	0.9393	1.0000	1.0838
$r^{*\prime}(1)$	0.5536	0.3914	0.2839	0.2344	0.2090	0.2044	0.1993
r_{Ns} (g N/m^3 day)	58,604.9	80,581.7	96,012.3	103,976.5	108,837.7	109,877.0	111,147.2
I	0.5979	0.6535	0.7028	0.7288	0.7333	0.7266	0.6636
ϕ^2	15.511	10.660	7.261	5.505	4.432	4.203	3.923
ρ	0.7384	0.7720	0.8006	0.8153	0.8178	0.8140	0.7547
ϕ^*	5.335	4.231	3.366	2.877	2.574	2.518	2.625
d	0.3964	0.5528	0.6512	0.7013	0.7320	0.7291	0.7824
η	0.187	0.236	0.297	0.348	0.388	0.397	0.381
r_{ob} (N) (g N/m^3 day)	10,959.1	19,017.3	28,515.6	35,456.0	41,576.0	43,621.2	42,347.1
r_{bio} (g biomass/m^3 h)	68.49	118.86	178.22	221.60	259.85	272.60	264.70

(*) At this ammonium concentration, oxygen is the limiting substrate. $C_{Ns} > 13.84$ g of N/m^3.
r_{Ns} (g N/m^3 day): rate of ammonium consumption evaluated on the biofilm–fluid interface.
r_{ob} (N) (g N/m^3 day): net rate of ammonium consumption in the biofilm.
r_{bio} (g biomass/m^3 h): net rate of biomass growth in the biofilm.

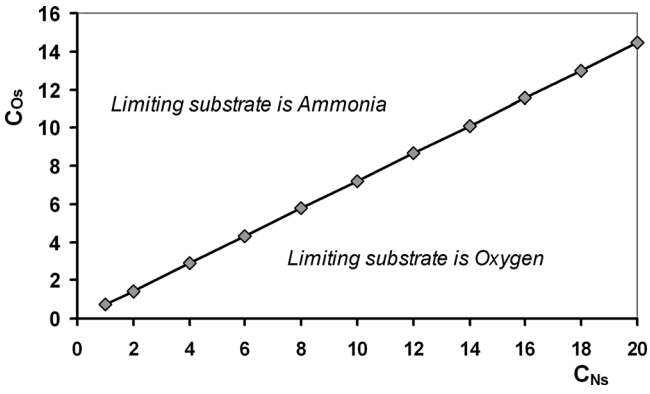

Figure 4. Oxygen and ammonia biofilm–fluid interface concentrations that delimit the zones where each one is the limiting substrate for the test case.

the biofilm) whenever

$$\Gamma_O = (1 - Y_N)\frac{C_{Ns}\bar{D}_{fN}}{C_{Os}\bar{D}_{fO}} \leq 1 \tag{44}$$

Therefore, ammonium will be the limiting component for $C_{Ns} \leq 13.84$ g of N/m^3. At these concentrations ammonium is limiting inside the biofilm, but oxygen is fully penetrating it. Conversely, for $C_{Ns} > 13.84$ g of N/m^3, oxygen becomes the limiting component inside the biofilm and ammonium is fully penetrating it (Fig. 4).

Taking into account that

$$D^*_{fO}(x^* = 1) = \frac{D_{fO}(x = L_f)}{\bar{D}_{fO}} \quad \text{and} \quad D^*_{fN}(x^* = 1) = \frac{D_{fN}(x = L_f)}{\bar{D}_{fN}} \tag{45}$$

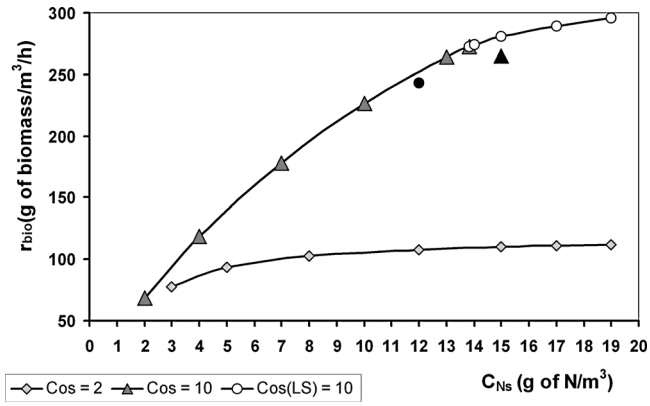

Figure 5. Observed (net) rate of biomass growth as a function of ammonium substrate concentration at two different oxygen concentrations. Points for $C_{0s} = 2$ correspond to Case I with oxygen as limiting substrate. Points C_{0s} (LS) correspond to conditions where oxygen is the limiting component in Case II. Black points correspond to calculations out of the range of the limiting component. Points at $C_{Ns} = 13.84$ g of N/m^3, ($\Gamma_O = \Gamma_N = 1$), $r_{bio} = 268.5$ g of biomass/m^3 of biofilm/h.

then for both cases

$$D^*_{fO}(x^* = 1) \approx D^*_{fN}(x^* = 1) \approx 1.5 \tag{46}$$

The assumption stated by Equation (20) that the diffusivity gradient ξ is constant for any of the substrates studied here is fulfilled; it holds not only at this point ($x^* = 1$), but for any value of x^*.

For Case I (low oxygen concentration), the net rate of biomass growth increases slowly as the ammonium concentration increases until it reaches a plateau when oxygen was consumed completely; therefore, the rate of biomass production cannot increase any more. The parameter values and rate equation indicated in Table II were used to calculate η according to Equation (33). In Case II (high oxygen concentration), the net rate of biomass formation increases constantly with ammonia concentration (Fig. 5). This increment is faster than in Case I since the amount of oxygen is sufficient to react with all the ammonium available in the biofilm. However, when the concentration of ammonium exceeds the value of 13.84 g of N/m^3, the rate of biomass formation begins to decrease and oxygen becomes the limiting substrate. Therefore, we must modify the calculation starting from this point, considering oxygen as the limiting substrate (for C_{Ns} values greater than 13.84 g of N/m^3) (points characterized as C_{Os}(LS) = 10 g of O_2/m^3 in Fig. 5).

To look for internal consistency of the method, calculations were performed for Case II with ammonium concentrations higher than the maximum accepted ($C_{Ns} > 13.84$ g of N/m^3). Results are shown in Table IV (oxygen is the limiting substrate inside the biofilm) and represented in Figure 5. The profile of the observed reaction rate of biomass growth as a function of ammonium concentration has continuity along the full range of ammonium concentrations, although at the point $C_{Ns} \geq 13.84$ g of N/m^3 the limiting substrate changes (oxygen begins to be the limiting substrate inside the biofilm).

We also calculated the net rate of biomass formation in the region where oxygen, and not ammonium anymore, is the limiting substrate ($C_{Ns} \geq 13.84$ g of N/m^3), at $C_{Ns} = 15$ g of N/m^3. If we consider in this case ammonium as the limiting substrate, the deviation of the point from the curve is clearly observed (black triangle in Fig. 5). Looking at Table III, parameter Γ_O is greater than 1, which means that the limiting component is not anymore the selected one (ammonium). The same behavior is observed when considering oxygen the limiting component at a C_{Ns} concentration lower than 13.84 g of N/m^3 (Table IV, for $C_{Ns} = 12$ g of N/m^3, $\Gamma_N > 1$). The circle black point in Figure 5 represents this calculation.

Continuing with Case II, the calculation for $C_{Ns} = 13.84$ g of N/m^3 can be carried out considering either oxygen or ammonium as the limiting compound inside the biofilm (Equation 42). Tables III and IV list the values of the net rate of biomass formation calculated considering ammonium and oxygen as the limiting component, respectively, for the keystone ammonium concentration of $C_{Ns} = 13.84$ g of N/m^3.

Table IV. Calculated parameters for test Case II ($C_{0s} = 10$ g of O_2/m^3): oxygen-limited process ($C_{Ns} > 13.84$ g of N/m^3).

	C_{Ns} (g/m^3)					
Parameters	12 (*)	13.84	14	15	17	19
β_N	0.2000	0.1734	0.1714	0.1600	0.1412	0.1263
Γ_N	1.1533	1.0000	0.9886	0.9227	0.8142	0.7285
$r^{*\prime}(1)$	0.2488	0.2044	0.2012	0.1839	0.1573	0.1383
r_{Os} (g O_2/m^3 day)	91,326	93,395.5	93,553.5	94,475.2	96,033.5	97,300.6
I	0.5909	0.7266	0.7327	0.7628	0.7988	0.8195
ϕ^2	4.110	4.203	4.210	4.251	4.322	4.379
ρ	0.7341	0.8141	0.8175	0.8340	0.8535	0.8645
ϕ^*	2.761	2.518	2.510	2.472	2.436	2.420
d	0.743	0.7403	0.7423	0.7548	0.7803	0.8019
η	0.362	0.397	0.398	0.404	0.410	0.413
r_{ob} (O_2) (g O_2/m^3 day)	33,060.0	37,078.0	37,234.3	38,168.0	39,373.7	40,185.2
r_{bio} (g biomass/m^3 h)	243.1	272.6	273.8	280.6	289.5	295.5

(*) At this ammonium concentration, ammonium is the limiting substrate. $C_{Ns} < 13.84$ g of N/m^3.
r_{Os} (g O_2/m^3 day): rate of oxygen consumption evaluate on the biofilm–fluid interface.
r_{ob} (O_2) (g O_2/m^3 day): net rate of oxygen consumption in the biofilm.
r_{bio} (g biomass/m^3 h): net rate of biomass growth in the biofilm.

The value of the net rate of biomass growth is the same (268.4 g biomass/m^3/h) using either of the two different approaches.

The method presented to calculate the net rate of biomass growth in a continuum biofilm with variable effective diffusivities and density, and a Double-Monod kinetic expression, is very fast and precise. It is important to pay attention to the values of the parameters Γ_O and Γ_N, or Equation (42), to know which substrate is the limiting one inside the biofilm, in the region where the calculation is carried out.

Discussion

Numerical outcomes using a rigorous and highly time intensive numerical method have shown that our estimation procedure predicts η values in very close agreement with the corresponding numerical finding, for the entire range of Thiele modulus values ($0 < \phi < \infty$). Similar results were obtained previously for single substrate limitation kinetics (Gonzo et al., 2012).

Other studies have considered dual-substrate kinetics. Recently, Olivieri et al. (2011) modeled an aerobic biofilm reactor with double-limiting substrate kinetics. The model describes the evolution of both the suspended cells and biofilm growth in a three-phase biofilm reactor. In the case studied by Olivieri et al. (2011), the biofilm grows on small spherical non-porous particles (300 μm diameter). The authors considered that the mass transfer between the liquid phase and the solid biocatalyst is large enough compared to the mass transport and conversion within the biofilm to render the external mass transfer resistance insignificant. Therefore, the substrate bulk fluid concentrations are equal to the concentrations on the fluid/biofilm interface. As in our case, they used the equation of Fan et al. (1990) to relate the substrate effective diffusivities with the biomass concentration. They solved the mass balance differential equation using a variable step continuation algorithm implemented in MATLAB® based on a predictor-corrector method, to obtain the biofilm efficiency factor η. However, the authors considered substrate effective diffusivities as well as biofilm density constant within the biofilm, in contrast to our approach.

A comparison of a minimum-rate (this model assumed that one of the two substrates controlled substrate utilization and biomass growth, hence single Monod kinetics apply) and a multiplicative Monod biodegradation kinetic model was carried out by Odencrantz (1992). General guidelines were based on the relation of the ratio between the half-velocity coefficients and substrate concentrations to establish which model is suitable for a particular problem. Strong simplifications were introduced to approach first to zero-order kinetics to analyze the differences between both types of kinetic expressions. The study assumed homogeneous biofilms.

Qi and Morgenroth (2005) presented a systematic analysis of a steady-state biofilm model for the multiplicative utilization of an electron donor and electron acceptor (dual-substrate limitations). The external and internal mass transport resistance effects on the rate of substrate consumption were considered. However, an important simplification was introduced by setting a constant biofilm thickness and density to solve the substrate mass balance differential equations. By assuming that the overall growth rate and overall rate of biomass loss from detachment are equal, and that the biofilm thickness remains constant, the authors could partially solve the dual-substrate model analytically. Substrate fluxes as well as their concentration profiles were thus obtained inside the biofilm.

Our pseudo-steady-state assumptions differ from those of Qi and Morgenroth (2005), because in the model we decouple biofilm growth from diffusion and biological

reaction processes. This is possible due to the characteristic short-time scales of diffusion and substrate utilization reactions compared to those of biomass growth and loss. The procedure gives estimates of the effectiveness factor to obtain the observed rate of biomass production for a fixed biofilm thickness. We assume pseudo-steady state for the diffusion-reaction process, but not steady-state biofilm growth. It is necessary to know both the rate of biomass production and the rate of biofilm loss to solve for the biofilm growth rate (dL_f/dt). In contrast, the steady-state biofilm model ($dL_f/dt = 0$) as defined by Qi and Morgenroth (2005) and in many other publications, is only supportable if the rate of biomass growth equals the rate of loss due to cell death and detachment.

Rittmann and Manem (1992) described two different schemes to do a mass balance of biomass. One method allows the layer to change in size, holding the total biomass density constant, but letting the volume of the layer increase or decrease when total biomass changes. The second method allows biomass flux between layers of fixed size. Using biomass flux may require that new layers be created if there is biomass "spill-over" to the outermost layer. This simplifying assumption then allows the modeler to find the relations between substrate concentrations inside the biofilm.

In all these previous works, the substrate effective diffusivities as well as biofilm density were considered independent of the biofilm thickness (i.e., they are constant inside a homogeneous biofilm). In contrast, in the present study, the fundamental assumption is to consider the variation of effective diffusivity across the biofilm, ξ, constant for any of the substrates. This assumption allows one to obtain the relation between substrate concentrations as the ratio between effective diffusivities, stoichiometric coefficients, and substrate concentrations at the biofilm–fluid interface. Once this relation is obtained the dimensionless rate of biomass production is a function of the concentration of the limiting substrate only. Therefore, the mass balance differential equations of the substrates can be solved considering one differential equation (limiting component) and linear relations to obtain the concentration of the other substrates. By applying the perturbation and matching technique previously developed (Gonzo et al., 2012), the effectiveness factor of the system is found and, consequently, the net rates of biomass production or substrate consumption are determined. The substrate fluxes through the biofilm–fluid interface are easily calculated. The procedure was extended to consider a system where n ($n > 2$) limiting substrates influence the kinetics of the biofilm growth and presents a comprehensive analytical approach towards solving multi-substrate kinetics. Possible external mass transfer limitations are not considered in the model (see assumption f). However, if the conditions are such that external mass transfer limitations are important, the model can be easily extended to include the effect of the external mass transfer resistance under the given simplifying assumptions (Gonzo et al., 2012).

Conclusions

Many biological systems encounter several limiting substrates, generating a need for the development of models and approaches that can account for the heterogeneity in biofilm diffusivity and density. The mathematical model and the technique presented in this study successfully combine the prediction of the effectiveness factor, and consequently, the net rate of biomass production and/or the rate of utilization of the limiting substrates participating in the system, in a fast and effective way. The method considers a continuum heterogeneous model for the biofilm with variable effective diffusivities as well as biofilm densities as a function of biofilm thickness. The application of the method in a heterogeneous biofilm with multiple-substrate kinetics was demonstrated in two test cases by considering the role of each of the limiting substrates, the importance of selecting the limiting substrate in any case, and the calculation of the net rate of substrate consumption or biomass growth. We calculate the biomass production rate for a given value of the biofilm thickness. This procedure assumes pseudo-steady state for the diffusion-reaction process, but not steady-state biofilm growth. This means that no equilibrium between the overall rate of biomass growth in the biofilm and the overall rate of biomass loss via detachment and cell death is assumed. Hence, the method refers to the net rate of biofilm growth only and can be combined with any type of rate of biomass loss.

Nomenclature

a	parameter defined by Equation (29) (kg/m^3)
b	parameter defined by Equation (29) (kg/m^3)
C_i^*	dimensionless substrate (i) concentration defined by Equation (9)
C_i	concentration of substrate (i) (kg/m^3)
C_{is}	concentration of substrate (i) at the biofilm–fluid interface (kg/m^3)
c	dimensionless parameter defined by Equation (28)
D_{fi}	surface average effective diffusivity of substrate (i) (m^2/s)
D_{fi}^*	dimensionless relative effective diffusivity of substrate (i), defined by Equation (9)
$\bar{D}_{fi}$	average effective diffusivity of nutrient (i) in the biofilm (m^2/s)
D_{fi}°	relative effective diffusivity of substrate (i), defined by Equation (8)
D_{wi}	diffusivity of substrate (i) in the liquid medium (m^2/s)
d	dimensionless parameter defined by Equation (33)
I_m	dimensionless parameter defined by Equation (B-16)
K_i	Monod half rate constant for substrate (i) (kg/m^3)
L_f	average biofilm thickness (m)
n	number of substrates
q_{max}	maximum specific growth rate (s^{-1})
r	specific reaction rate (s^{-1})
r_s	reference reaction rate defined by Equation (10 or B-6)

r^* dimensionless rate of reaction defined by Equation (9)
$r^{*\prime}$ first derivative of r^* with respect to the limiting component
r_{iob} net rate of substrate (i) consumption of the whole biofilm (kg of substrate/s/m^3)
r_{bio} net biomass production rate (kg of biomass/m^{3}of biofilm/s)
S_x biofilm–fluid interface surface area (m^2)
X_f biofilm density (kg/m^3)
$\bar{X}_f$ average biofilm density along the (x) direction (kg/m^3)
X_f^* dimensionless relative effective diffusivity defined by Equation (9)
x distance from the bottom of the biofilm (m)
x^* dimensionless distance defined by Equation (9)
Y_i yield coefficient for substrate (i) (kg microorganism/kg nutrient)

Greek Letters

α_i effective diffusivity of substrate (i), at the bottom of the biofilm (m^2/s)
β_i dimensionless parameter for substrate (i) defined by Equation (9)
ϕ Thiele modulus. Equation (14) or (B-4)
ϕ^* normalized Thiele modulus, defined by Equation (34)
Γ_i parameter defined by Equations (15) and (B-3)
η effectiveness factor for a continuum heterogeneous biofilm
κ parameter defined by Equation (26)
ν_i ratio between the substrate (i) yield coefficient and that of the limiting substrate
ρ parameter defined by Equation (A-18)
ρ_m parameter defined by Equation (B-17)
σ parameter defined by Equation (A-9)
σ^* parameter defined by Equation (35)
σ_m parameter defined by Equation (B-13)
ξ effective diffusivity gradient (m/s)
Ψ parameter defined by Equation (25)

Sub Indexes

i for nutrient 1, 2, 3, …, A and B
s biofilm–fluid interface conditions
m for multiple limiting substrates
N ammonium
O oxygen

E.E.G. and V.B.R. gratefully acknowledge the financial support provided by CONICET and Universidad Nacional de Salta in Argentina as well as the Fogarty International Center at the University of California, Davis, USA. S.W. was supported by the Singapore Ministry of Education and National Research Foundation through an RCE award to Singapore Centre on Environmental Life Sciences Engineering (SCELSE).

References

Alhede M, Qvortrup K, Liebrechts R, Hofiby N, Givskov M, Bjarnsholt T. 2012. Combination of microscopic techniques reveals a comprehensive visual impression of biofilm structure and composition. FEMS Immun Med Microbiol 65:335–342.

Bae W, Rittmann BE. 1996. A structural model of dual-limitation kinetics. Biotechnol Bioeng 49:683–689.

Behrens S, Kappler A, Obst M. 2012. Linking environmental processes to the in situ functioning of microorganisms by high-resolution secondary ion mass spectrometry (NanoSIMS) and scanning transmission X-ray microscopy (STXM). Environ Microbiol 14:2851–2869.

Beyenal H, Lewandowski Z. 2000. Combined effect of substrate concentration and flow velocity on effective diffusivity in biofilms. Water Res 34:528–538.

Beyenal H, Lewandowski Z. 2002. Internal and external mass transfer in biofilms grown at various flow velocities. Biotechnol Prog 18:55–61.

Beyenal H, Lewandowski Z. 2005. Modeling mass transport and microbial activity in stratified biofilm. Chem Eng Sci 60:4337–4348.

Beyenal H, Tanyolac A, Lewandowski Z. 1998. Measurement of local effective diffusivity in heterogeneous biofilms. Water Sci Technol 38: 171–178.

Bischoff K, Froment G. 1980. Chemical Reactor Analysis and Design. New York: Wiley. 719 p.

Bungay HR. 1994. Growth rate expressions for two substrates one of which is inhibitory. J Biotechnol 34:97–100.

Collins G, Mahony T, Enright A-M, Gieseke A, de Beer D, O'Flaherty V. 2007. Determination and localisation of in situ substrate uptake by anaerobic wastewater treatment granular biofilms. Water Sci Technol 55:369–376.

Fan LS, Leyva-Ramos R, Wisecarver KD, Zehner BJ. 1990. Diffusion of phenol through a biofilm grown on activated carbon particles in a draft-tube 3-phase fluidized-bed bioreactor. Biotechnol Bioeng 35:279–286.

Gonzalez BC, Spinola AL, Lamon AW, Araujo JC, Campos JR. 2011. The use of microsensors to study the role of the loading rate and surface velocity on the growth and the composition of nitrifying biofilms. Water Sci Technol 64:1607–1613.

Gonzo EE, Gottifredi JC. 2007. A simple and accurate method for simulation of hollow fiber biocatalyst membrane reactors. Biochem Eng J 37:80–85.

Gonzo EE, Wuertz S, Rajal VB. 2012. Continuum heterogeneous biofilm model. A simple and accurate method for effectiveness factor calculation. Biotechnol Bioeng 109(7):1779–1790.

Gottifredi JC, Gonzo EE. 1986. Application of perturbation and matching techniques to solve transport phenomena problems. In: Mujumdar AS, Mashelkar RA, editors. Advances in transport processes, Vol. IV. New Delhi: Wiley Eastern Limited. p 419–464.

Kofoed MV, Nielsen DÅ, Revsbech NP, Schramm A. 2012. Fluorescence in situ hybridization (FISH) detection of nitrite reductase transcripts (nirS mRNA) in *Pseudomonas stutzeri* biofilms relative to a microscale oxygen gradient. Sys Appl Microbiol 35:513–517.

Lewandowski Z, Beyenal H. 2003. Mass transport in heterogeneous biofilms. In: Wuertz S, Bishop P, Wilderer P, editors. Biofilms in wastewater treatment. An interdisciplinary approach. London: IWA Publishing. p 147–177.

Lewandowski Z, Beyenal H, Myers J, Stookey D. 2007. The effect of detachment on biofilm structure and activity: The oscillating pattern of biofilm accumulation. Water Sci Technol 55:429–436.

Neu TR, Manz B, Volke F, Dynes JJ, Hitchcock AP, Lawrence JR. 2010. Advanced imaging techniques for assessment of structure, composition and function in biofilm systems. FEMS Microb Ecol 72(1):1–21.

Nielsen PH, Nielsen JL. 2005. Microautoradiography: Recent advances within the studies of the ecophysiology of bacteria in biofilms. Water Sci Technol 52(7):187–194.

Noguera DR, Pizarro G, Stahl DA, Rittmann BE. 1999. Simulation of multispecies biofilm development in three dimensions. Water Sci Technol 39(7):123–130.

Odencrantz JE. 1992. Comparison of minimum-rate and multiplicative Monod biodegradation kinetic models applied to *in situ* bioremediation. Proceedings of Solving Ground Water Problems with Models, IGWC, February 1992, Texas, USA.

Olivieri G, Russo ME, Marzocchella A, Salatino P. 2011. Modeling of an aerobic biofilm reactor with double-limiting substrate kinetics: Bifurcational and dynamic analysis. Biotechnol Prog 27:1599–1613.

Picioreanu C, Kreft JU, van Loosdrecht MCM. 2004. Particle-based multidimensional multispecies biofilm model. Appl Environ Microbiol 70:3024–3040.
Qi S, Morgenroth E. 2005. Modeling steady-state biofilms with dual-substrate limitations. J Environ Eng 131:320–326.
Rittmann BE, Manem JA. 1992. Development and experimental evaluation of a steady-state, multi-species biofilm model. Biotechnol Bioeng 39: 914–922.
Wanner O. 1995. New experimental findings and biofilm modeling concepts. Water Sci Technol 32:133–140.
Wanner O, Eberl H, Morgenroth E, Noguera D, Picioreanu C, Rittmann B, van Loosdrecht M. 2006. Mathematical modeling of biofilms. London: IWA Publishing. 179 p.
Wanner O, Gujer W. 1986. A multispecies biofilm model. Biotechnol Bioeng 28:314–328.
Wu S, Shih S, Liu H. 2007. Dynamic behavior of double-substrate interactive model. J Chinese Inst Chem Eng 38:107–115.
Wuertz S, Bishop P, Wilderer P. 2003. Biofilms in wastewater treatment. An interdisciplinary approach. London: IWA Publishing. 401 p.
Zienkewicz OC, Taylor LR. 1991. The finite element method. London: McGraw-Hill. 30 p.

Supporting Information

Additional supporting information may be found in the online version of this article at the publisher's web-site.